Journal of the Optical Society of Korea
Vol. 12, No. 4, December 2008, pp. 262-268

DOI: 10.3807/JOSK.2008.12.4.262

# Optical Design of A Compact Imaging Spectrometer for STSAT3

Jun Ho Lee*

*Department of Optical Engineering, Kongju National University, 314-701, Korea*

Tae Seong Jang

*Satellite Technology Research Center, KAIST, 305-701, Korea*

Ho-Soon Yang

*Korea Research Institute of Standards and Science, 305-340, Korea*

Seung-Wu Rhee

*Korea Aerospace Research Institute, 305-333, Korea*

(Received November 11, 2008 : accepted December 1, 2008)

A compact imaging spectrometer (COMIS) for use in the STSAT3 microsatellite is currently under development. It is scheduled to be launched into a low Sun-synchronous Earth orbit (~700 km) by the end of 2010. COMIS was inspired by the success of CHRIS, which is a small hyper-spectral imager developed for the ESA microsatellite PROBA. COMIS is designed to achieve nearly equivalent imaging capabilities of CHRIS in a smaller (65 mm diameter and 4.3 kg mass) and mechanically superior (in terms of alignment and robustness) package. Its main operational goal will be the imaging of Earth's surface and atmosphere with ground sampling distances of ~30 m at the 18~62 spectral bands (4.0~1.05 μm). This imaging will be used for environmental monitoring, such as the in-land water quality monitoring of Paldang Lake, which is located next to Seoul, South Korea. The optics of COMIS consists of two parts: imaging telescope and dispersing relay optics. The imaging telescope, which operates at an f-ratio of 4.6, forms an image (of Earth's surface or atmosphere) onto an intermediate image plane. The dispersion relay optics disperses the image and relay it onto a CCD plane. All COMIS lenses and mirrors are spherical and are made from used silica exclusively. In addition, the optics is designed such that the optical axis of the dispersed image is parallel to the optical axis of the telescope. Previous efforts focused on manufacturing ease, alignment, assembly, testing, and improved robustness in space environments.

*Keywords*: Imaging spectrometer, STSAT3, Space optics

*OCIS codes* : (080.3620) Lens design; (120.4570) Optical design of instruments; (220.4830) Optical systems design; (300.6190) Spectrometers, (350.6090) Space optics

## I. INTRODUCTION

STSAT3 is a ~150 kg microsatellite for technical demonstrations and scientific observations. The former includes investigations of multi-functional composite structures and hall-thrusters. The latter is to provide IR imaging of the Galaxy (at 1-2 μm wavelengths) and hyper-spectral imaging of Earth's surface (in the visible and near IR bands at 0.4~1.05 μm wavelengths). The hyper-spectral imaging will focus on the Korean Peninsula [1]. A schematic diagram of the STSAT-3 operational considerations is shown in Figure 1. Figure 2 presents a deployed view of STSAT3; the COMIS hyper-spectral imager is a secondary payload and is indicated by the

*Corresponding author: jhlsat@kongju.ac.kr

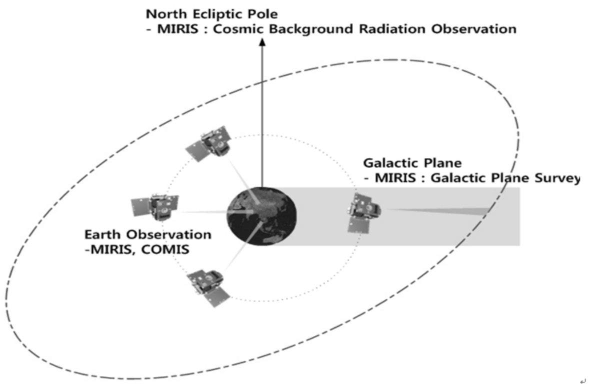


FIG. 1. Operational concept of STSAT-3.

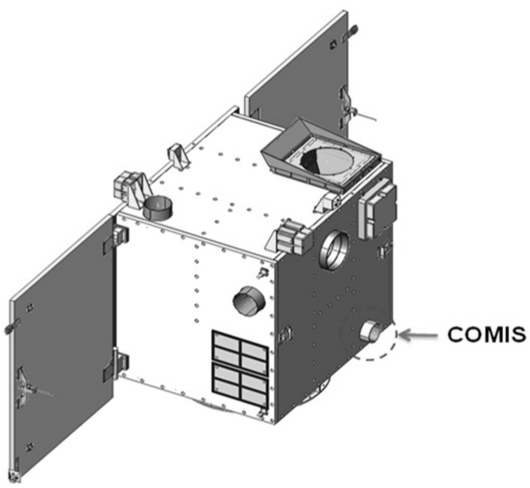


FIG. 2. Deployed STSAT3 model indicating COMIS with a dashed circle.

dashed circle.

COMIS was inspired by the success of CHRIS, which is a small hyper-spectral imager developed for the ESA microsatellite PROBA [2,3]. COMIS is designed to achieve nearly equivalent imaging capabilities of CHRIS in a smaller (65 mm diameter and 5 kg mass) and mechanically superior (in terms of alignment and robustness)

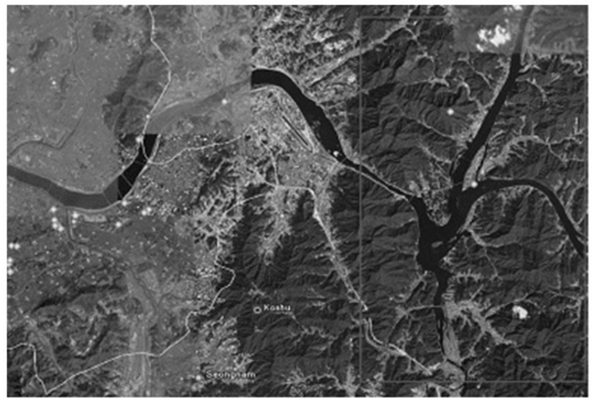

FIG. 3. One mission of COMIS is for in-land water quality monitoring of Paldang Lake (red-box) next to Seoul, South Korea.

package. COMIS is capable of hyper-spectral imaging at 30 m or less ground sampling distances (GSDs) over a 30 km swath at an altitude of 700 km. The number of bands is adjustable (18-62). A major scientific application of COMIS is environmental monitoring, such as in-land water quality monitoring of Paldang Lake located next to Seoul, South Korea(Fig. 3).

## II. OPTICAL DESIGN OF COMIS

### 2.1 Concept

COMIS is a conventional imaging spectrometer consisting of imaging and dispersion relay optics. The imaging telescope forms an image (of Earth's surface) on an intermediate image plane. The dispersion relay optics disperse the image and relay it to a CCD. Since COMIS operates in a *push–broom* mode; the CCD rows are assigned to accommodate different wavelengths, and the CCD columns are assigned to separately resolved areas of an image (Earth's surface). Figure 4 shows the push-broom imaging mode used to scan Earth's surface as STSAT3 moves in its orbit. The required ground

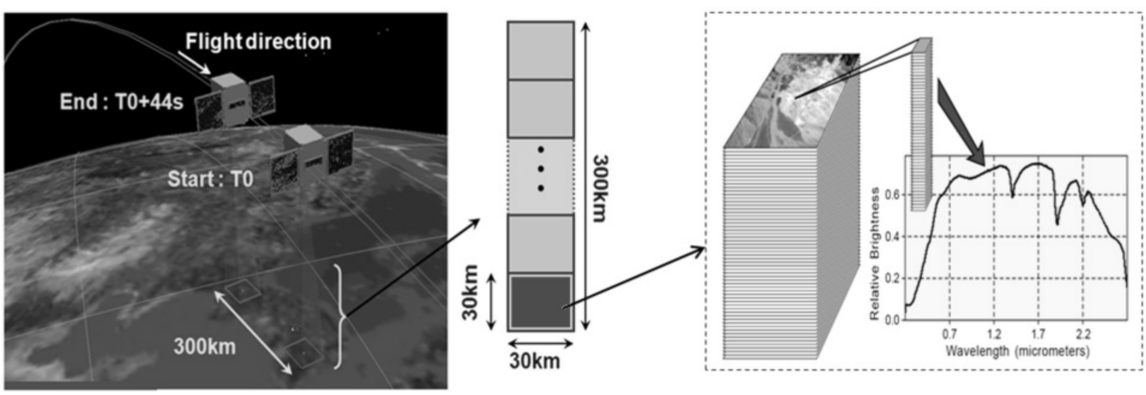


FIG. 4. The COMIS Strip imaging mode-one scene consists of 30 km by 30 km image of Earth at 18~62 wavebands.

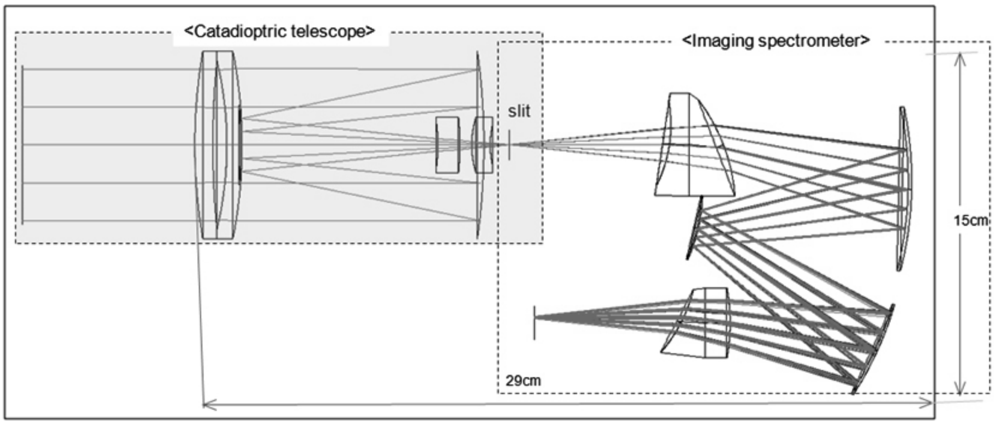


FIG. 5. Optical layout of COMIS comprising a catadioptric telescope and an imaging spectrometer.

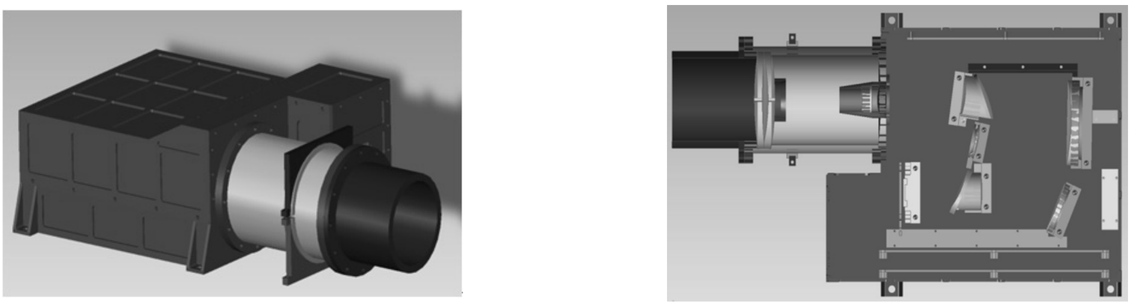

(a) 3D model of COMIS (b) Cross-sectional view of COMIS

FIG. 6. 3D model of COMIS structure

sampling distance of COMIS was 30 m or less. For the case of 30 m GSD, one scene is defined as 1024 GSDs ×1024 GSDs, i.e. 30 km×30 km.

The spectral waveband covered by the instrument is limited to the 400-1050 nm band, which can be achieved using a single CCD detector. The CCD image size is 13.3×13.3 $mm^2$ at a 1024×1024 image format.

### 2.2 Design of the Imaging Telescope

The optical design is presented in Figure 5; its details are tabulated in Table 1. COMIS comprises a catadioptric telescope and an imaging spectrometer. Figure 6 shows the 3D model of COMIS.

The catadioptric telescope images a 27.3 m×28 km area of Earth's surface onto a slit of dimensions 11.8 μm×12.1 mm. This corresponds to a ground sampling distance of 27.3 m and a swath width of 28 km for nadir looking posture at an altitude of 700 km. The telescope has an entrance pupil diameter of 65 mm, operating at a focal length of 300 mm (f/4.6). The telescope is a conventional two-mirror telescope with four weak lenses. The two front meniscuses compensate for spherical aberrations and the two latter lenses (near to the slit plane) compensate for minor residual aberrations. The imaging telescope gives nearly diffraction-limited performance for all wavelengths and fields as shown in the spot diagram in Figure 7 and the modulation transfer function (MTF) plot in Figure 8.

Our telescope design adopts a single-material athermalization approach. Thus, the lenses, mirrors, and structures are all made of the same fused-silica material, which is both radiation hardened and relatively non-susceptible to thermal expansion. Details of the mechanical designs will be fully dealt in a separate paper [4].

### 2.3 Design of the Imaging Spectrometer

The imaging spectrometer disperses light from the slit and reimages it onto a CCD. It is essentially a modified Offner relay with two dispersing prisms (patented by Sira Electro-Optics Ltd) [5]. Our modifications make the optical axis of the entrance and exit beams parallel to that of the imaging telescope (Fig. 4). This eases alignment difficulties and makes the optics less sensitive to thermal contraction and expansion of the mechanical housing. Further modifications include magnification of the relay, which was increased from 1 to 1.1 in order to optimize optical performance in line with all spherical surfaces.

The main functions of the imaging spectrometer are relay and dispersion. Relay is handled by the Offner configuration (convex-concave-convex mirrors), whilst dispersion is handled by two curved prisms, which are

TABLE 1. Optical Data of COMIS in the ZEMAX format (unit: distance in mm, angle in deg.).

| Surf | Type | Radius | Thickness | Glass | Decenter Y | Tilt X |
|---|---|---|---|---|---|---|
| OBJ | STANDARD | Infinity | Infinity | | | |
| 1 | STANDARD | Infinity | 70.00 | | | |
| STO | STANDARD | 247.00 | 7.34 | SILICA | | |
| 3 | STANDARD | 395.00 | 1.64 | | | |
| 4 | STANDARD | Infinity | 4.05 | | | |
| 5 | STANDARD | -162.00 | 6.17 | SILICA | | |
| 6 | STANDARD | -215.00 | 96.70 | | | |
| 7 | STANDARD | -300.00 | -96.70 | MIRROR | | |
| 8 | STANDARD | -215.00 | 79.57 | MIRROR | | |
| 9 | STANDARD | -75.00 | 9.00 | SILICA | | |
| 10 | STANDARD | -120.00 | 4.79 | | | |
| 11 | STANDARD | 42.70 | 7.50 | SILICA | | |
| 12 | STANDARD | 39.50 | 0.82 | | | |
| 13 | STANDARD | Infinity | 7.00 | | | |
| 14 | STANDARD | Infinity | 65.00 | | | |
| 15 | STANDARD | -60.00 | 22.00 | SILICA | | 8.10 |
| 16 | STANDARD | -80.00 | 75.08 | | | -20.00 |
| 17 | STANDARD | -161.30 | -85.31 | MIRROR | -18.92 | 1.20 |
| 18 | STANDARD | -74.90 | 71.90 | MIRROR | -35.65 | 12.45 |
| 19 | STANDARD | -153.50 | -59.00 | MIRROR | -87.80 | 23.60 |
| 20 | STANDARD | -85.50 | -20.00 | SILICA | -76.08 | |
| 21 | STANDARD | -65.12 | -59.63 | | | 26.30 |
| IMA | STANDARD | Infinity | | | | |

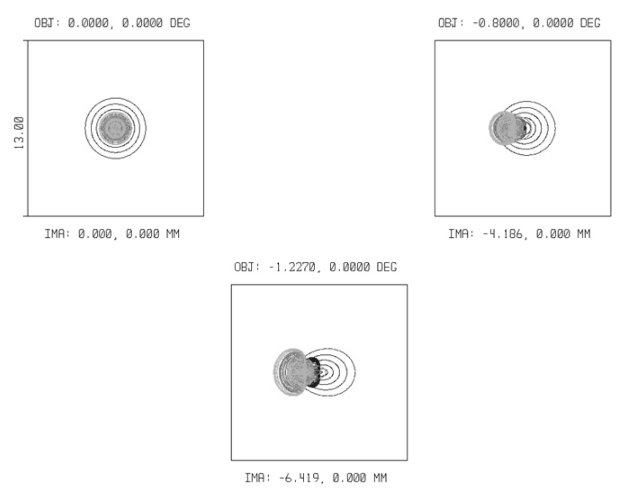


FIG. 7. Spot diagram of the COMIS imaging telescope showing all spots formed by the imaging optics within a single CCD pixel.

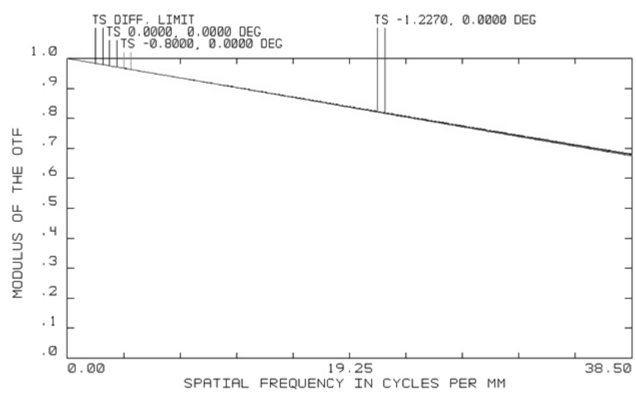


FIG. 8. MTF Plot of the COMIS imaging telescope showing the MTFs for all wavelengths and fields are nearly diffraction limited.

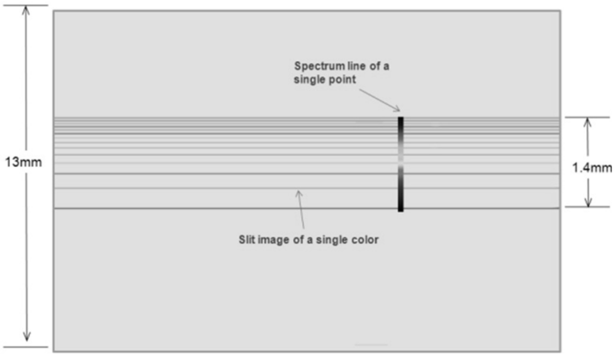


FIG. 9. Images of the entrance slit on the CCD plane while each line is a monochromatic image of the entrance slit.

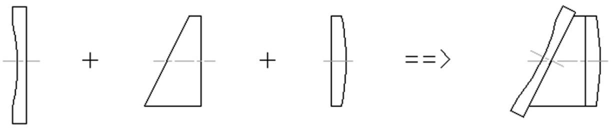


FIG. 10. Construction of a curved prism with two lenses and a prism

- 1024 by 1024 1:1 Image Format
- Image Area 13.3 x 13.3 mm
- Back Illuminated Format
- Frame Transfer Operation
- 13 μm Square Pixels
- Symmetrical Anti-static Gate Protection
- Very Low Noise Output Amplifiers
- Gated Dump Drain on Output Register
- 100% Active Area
- Advanced Inverted Mode Operation (AIMO)

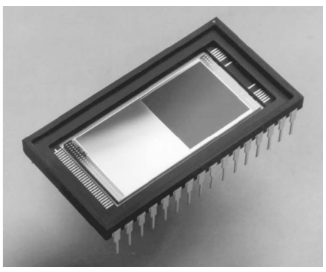

FIG. 11. The e2V CCD 47-20 detector [6].

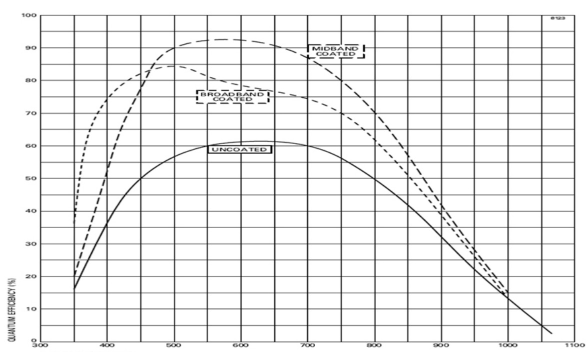


FIG. 12. Quantum efficiency of the detector used (e2V CCD 47-20) [6]

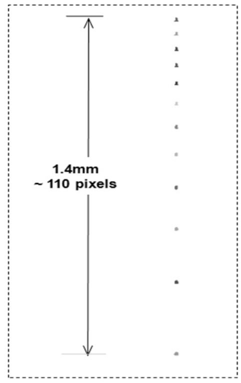


(a) Dispersion of 50 nm spaced spectrum

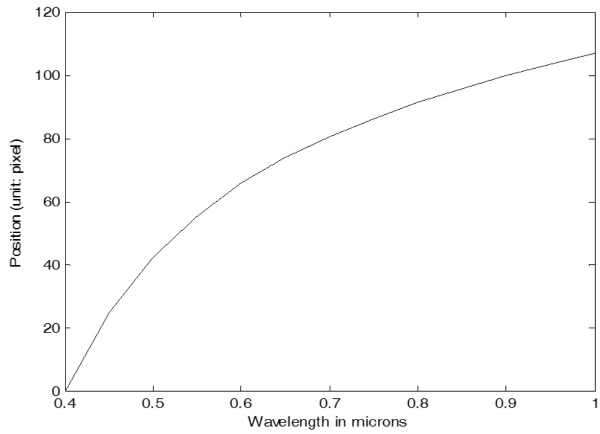


(b) Position of spectrum in the CCD plane in the unit of pixels

FIG. 13. Dispersion of a 50 nm spaced and its position on the CCD plane.

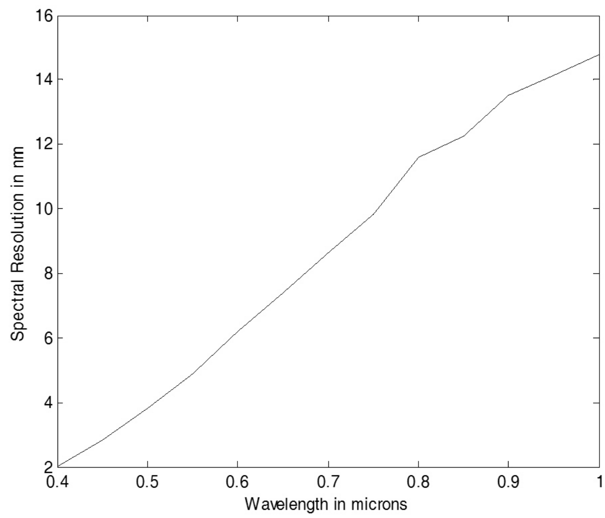


FIG. 14. Spectral resolutions over a single CCD pixel.

placed in the paths between both the entrance slit and first mirror as well as third mirror and detector. The optics relays and disperses the slit image onto the detector thereby producing a monochrome image of the entrance slit formed on each row of detector elements. The spectrum of each point in the row is imaged along a detector column (Fig. 9).

The dispersing prism has spherical surfaces in order to allow for correction of optical aberrations in diverging and converging beams. A single curved prism is con-

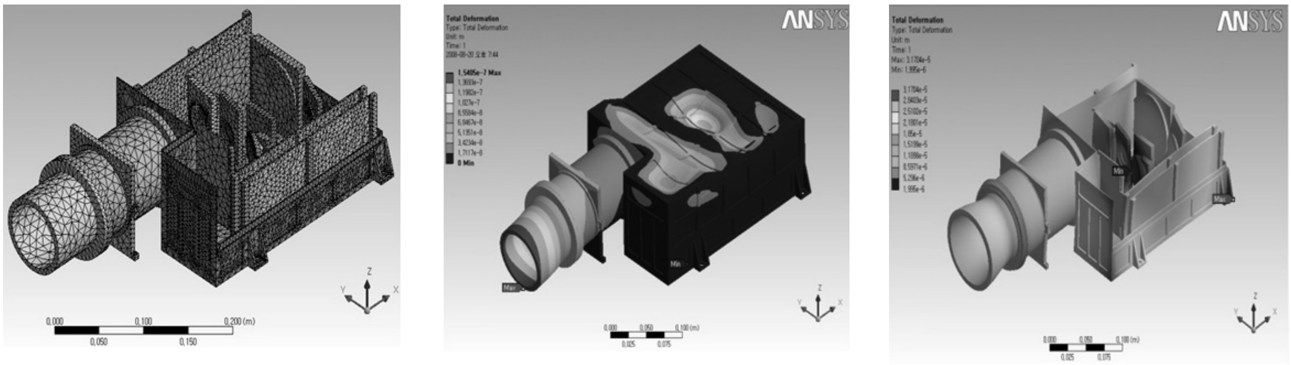

(a) FEA model (b) Gravity deformation (c) Thermal deformation

FIG. 15. FEA Model of COMIS and some results [4].

TABLE 2. Manufacturing tolerances for the COMIS optics.

| Item | Tolerances |
|---|---|
| Height | -10 ~ -30 microns |
| Thickness/Distance | ±20 microns |
| Centering | ± 1 arcmin |
| Spherical & Astigmatism | 0.1 fringe |
| Radius of curvature | ± 2 fringe |

structed from two lenses and a prism in order to ease manufacturing difficulties (Fig. 10).

### 2.4 Detector

The dispersed slit images are imaged onto the planar CCD detector, which is an e2V CCD type (CCD47-20) frame transfer device with 1024 rows and 1024 columns. A single pixel has the dimensions 13 μm×13 μm. Figure 12 illustrates the quantum efficiency of the CCD. The CCD (with broadband coating) offers high quantum efficiency over the visible and near IR allowing radiometric measurements in the spectral range 400-1050 nm.

## III. PERFORMANCE ANALYSIS

### 3.1 Spectral Resolution

Since we use prismatic dispersion power to disperse the spectral band, the spectral resolution varies depending on the refractive index of the prism. The spectral dispersion is non-linear due to dispersion of the refractive index of the prism as shown in Figure 13. The 400~1050 nm spectrum covers 1.4 mm of a CCD row i.e. ~110 pixels (Fig. 13). The corresponding spectral resolution over a single CCD pixel varies from 2 nm to 15 nm across the spectrum (Fig. 14).

### 3.2 System MTF

The COMIS system MTF takes into account contributions from optical design (diffraction, obstruction, and aberration), manufacturing and alignment, instabilities, detector integration, satellite flight (linear motion and jitter), and so on. MTF values for manufacturing and Assembly/Integration/Test (AIT) were predicted by Monte Carlo analysis using commercially available software (ZEMAX) with the tolerances given in Table 2. Decreases in MTF (due instabilities inherent in space flight, such as thermal expansion and zero gravity environ-

TABLE 3. System MTF budgets for COMIS optics.

| Item | | MTF@ 38.5 lpm | Note |
|---|---|---|---|
| Design MTF | | 0.63 | Diffraction + Aberration + Obstruction |
| Manufacturing | Imaging Telescope | 0.98 | Manufacturing + Assembly + Integration + Testing |
| | Imaging Spectrometer | 0.98 | |
| Instability in space | Imaging Telescope | 0.90 | Gravity Release + Thermal Expansion/Contraction |
| | Imaging Spectrometer | 0.85 | |
| Detector Integration | | 0.64 | 1 pixel (38.5lpm) |
| Linear motion | | 0.98 | 0.1 pixel movement over a pixel CCD integration time |
| Jitter | | 0.99 | 0.014 pixel random vibration over CCD integration |
| Resultant System MTF | | 0.29 | |

ments) were also predicted by the finite element analysis (FEA) of the COMIS mechanical model [4]. The effects of detector integration, linear motion, and jitter are predicted by the following equations:

a. detector integration, $MTF_{detector}=|\mathrm{sinc}(\xi x^{\cdot}p)|$ (1)

b. linear motion, $MTF_{linear\ motion})=|\mathrm{sinc}((\xi(\Delta V)\ )T|$ (2)

c. jitter, $MTF_{Jitter}=\exp\{-2\pi^2 a_{jitter}{}^2\xi^2\}$ (3)

where $\xi$ is the spatial frequency on the detector plane in lines-per-mm, $x_P$ the detector pitch, $\Delta V$ is x-component of the velocity vector scaled to focal plane coordinates, T is the integration time, and $\alpha_{jitter}$ is the observed random vibration profile scaled to focal plane coordinates [7,8]. The values for linear motion and jitter supplied from the STSAT3 bus developer are $\pm 0.052^o$/sec and $\pm 0.007^o$/sec, respectively. Table 3 summarizes the MTF calculation at the Nyqust frequency of the CCD detector (38.5 lines-per-mm). The resulting system MTF is 0.29.

## IV. CONCLUSION

The paper presents the optical design of a Compact Imaging Spectrometer (COMIS) for use in STSAT3. The Optical design consists of an imaging telescope (f/4.6) and an imaging spectrometer (1.1 magnification ratio). The combined optics are able to take hyperspectral images of Earth's surfaces at ~27.3 m GSD over 28 km for nadir looking posture at an altitude of 700 km. The spectral resolution of COMIS over a single pixel varies from 2 nm to 15 nm depending on the wavelength. The system MTF of COMIS is expected to be 0.29 considering the design, manufacturing and assembly errors, and operational hindrances in space environments. A COMIS prototype is currently being assembled and tested. Its investigation and modification will be based on the results of optical, mechanical, and space environment tests as applied to COMIS.

## ACKNOWLEDGMENT

This work is funded by the Ministry of Education, Science and Technology, South Korea.

## REFERENCES

[1] J. H. Lee, C. W. Lee, K. I. Kang, et. al, "A Compact Imaging Spectrometer (COMIS) for the Microsatellite STSAT3," *Proc. SPIE*, vol. 6744, pp. 67551C-1-8, 2007.

[2] M. J. Barnsley, J. J. Settle, M. A. Cutter, D. R. Lobb, and F. Teston, "The PROBA/CHRIS Mission: A Low-Cost Smallsat for Hyperspectral Multiangle Observations of the Earth Surface and Atmosphere," *IEEE Transactions on geosciences and remote sensing*, vol. 42, no. 7, pp. 1512-1520, 2004.

[3] M. A. Cutter, D. R. Lobb, and R. A. Cockshott, "Compact High Resolution Imaging Spectrometer (CHRIS)," *Acta Astronautica*, vol. 46, no. 2, pp. 262- 268, 2000.

[4] J. H. Lee, Y. M. Kim, and J. W. Kim, "Optomechanical Design of Compact Imaging Spectrometer (COMIS)," *J. Opt. Soc. Korea*, will be submitted.

[5] D. R. Lobb, "Imaging Spectrometer," US patent 6,288, 781 B1, 2001.

[6] www.2ev.com

[7] R. A. Schowengerdt, "Remote Sensing," Elsevier, 2007

[8] Jong-hoon Lee, J. H. Lee, and Yee-Jin Cheon, "Development of an Earth Observation Optical Payload Simulator," *Bull. Kor. Spac. Soc.*, vol. 17, no. 2, pp. 35, 2008.